The effect of Mn-Co-Ti dopants on the magnetic properties, Complex permittivity, permeability, and microwave absorbing characteristics of barium hexaferrite

MOHAMMAD H. SHAMS, AMIR S. H. ROZATIAN, MOHAMMAD H. YOUSEFI
Department of Physics, University of Isfahan, Hezar Jarib Street, Isfahan 81746-73441, Iran

In this research, doped barium M-type hexaferrites with the composition of $BaFe_{12-x}(MnCo)_{0.5x}Ti_{0.5x}O_{19}$ (x=1.5, 2, 2.5) were synthesized by the conventional ceramic method. The crystalline structure, particles size, magnetic properties, complex permittivity, complex permeability and microwave absorption properties were investigated by X-ray diffraction, Scanning Electron Microscope, Vibrating Sample Magnetometer and Vector Network Analyzer. The results showed that samples with the Magnetoplumbite structures and widely distributed particle sizes were formed. The coercive force and resonance absorption frequency of samples were reduced by raising the amount of Mn-Co-Ti dopants. The optimal reflection loss plots of composite samples in different frequency bands were calculated with a computer code to find the optimal thickness for each material based on the maximum reflection loss bandwidth for -10dB. It was also found that all samples showed good performance at C, X and Ku frequencies bands in terms of microwave absorption.

(Received April 16, 2015; accepted May 7, 2015)

Keywords: Microwave material, Barium hexaferrite, Magnetic properties, solid state ceramic method

1. Introduction

Electromagnetic wave pollution is produced by many new wireless systems such as smart homes, remote telemedicine, wireless sensors and military and civil radars [1]. Therefore, development of microwave absorbing materials has become necessary to overcome electromagnetic wave pollution. An absorbing material should be able to realize favourable loss in the necessary frequency range. This loss is originated in electric or electromagnetic phenomena. Thus, to achieve maximum loss in a vast frequency range, selecting the material and controlling its dielectric and magnetic properties are of high importance. So far, various materials have been studied to evaluate their capability of absorbing EM waves [2]. Among these materials, there are ferrites which are mostly applied due to their absorbing power. Ferrites, depending on its crystal structure and chemical composition, can be used in a special frequency range. For instance, spinel ferrites including MnZn and NiZn ferrites are mostly utilized in MHz ranges. Of course, due to Snoek limit, their absorbing power can be reduced. Another type of ferrites, called hexaferrites, is capable of higher absorbing power in GHz frequencies. Hexaferrites, depending on their chemical compositions, are divided into M, W, Y, U, X and Z-types [3]. Among hexaferrites, M-type with the formula $MFe_{12}O_{19}$ is the most applicable because of its high stability, efficient high frequency response, and switching properties. These materials are utilized in permanent magnets, magnetic recording media, and microwave absorbing materials [4]. The microwave absorbing mechanism in these compounds comes from the magnetic loss caused by the resonance phenomenon which originates from domain wall motions and spin relaxations (rotations). Anisotropic field in M-type ferrites, such as barium ferrite, is close to 1.36 MA/m, which corresponds to a natural resonance frequency of 47.6 GHz [5]. A recent extensive work has already been done to modify the magnetic parameters of M-type hexaferrites by substituting Fe3+ with other cations or cation combinations such as Co, Ni, Al, Co-Ti, Ru-Ti, Mg-Ti, Mn-Cd-Zr, Zn-Nb, Cr-Ga, Ni-Ti, etc. [1,6-13]. Proper selection of the dopant elements can determine the resonance frequency and the amount of absorption. It should be emphasized that in the previous works on the Mn-Co-Ti substituted barium hexaferrite [14-17], the microwave absorbing properties of only individual frequency bands have been studied.

This paper attempted to investigate in detail the structural and magnetic characteristics, complex permittivity and permeability and microwave absorbing properties of $BaFe_{12-x}(MnCo)_{0.5x}Ti_{0.5x}O_{19}$ as a function of the substituted amount of dopants in a range (x=1.5, 2, 2.5).

2. Experimental

2.1 The preparation of ferrite powders and composites samples

The M-type $BaFe_{12-x}(MnCo)_{0.5x}Ti_{0.5x}O_{19}$ (x=1.5, 2, 2.5) hexaferrites were synthesized by solid state reaction.

The raw materials used for obtaining the stoichiometric mixtures, with 99.9% purity, were barium carbonate ($BaCO_3$), iron oxide (Fe_2O_3), manganese carbonate ($MnCO_3$), cobalt oxide (Co_3O_4) and titanium oxide (TiO_2). To synthesize pure and doped stoichiometric hexaferrites, the starting materials were mixed in a ball mill for 2 h and sintered in air at 1230 °C for 1 h. The heating rates of samples were from the room temperature to 600 °C with 6 °C /min and they were kept at 3 °C /min to the final sintering temperature. Finally, the sintered hexaferrites were milled again in a fast mill for 6 h.

The composite specimens were prepared by homogeneously mixing the hexaferrite powders with 28 and 72 volume percent hexaferrite and paraffin wax, respectively. The mixtures were moulded to a toroidal shape with the outer diameter of 7.00 mm, the inner diameter of 3.04 mm, and the thickness of 1.5 mm.

2.2 Physical measurements

X-ray Diffraction (XRD) patterns were recorded on a X'Pert Pro MPD, PANalytical, X-ray diffractometer with Cu-Kα radiation (λ = 1.5406 Å) in the range of 20 to 70 degrees. Data were recorded with the steps of 0.026°. Electron micrographs were taken using a LEO435VP scanning electron microscope (SEM). The room temperature magnetization measurements up to a maximum field of 10 kOe were carried out using VSM M. D. K. Co. Iran. The scattering parameters in 0.3- 18 GHz were measured using a ZVK vector network analyzer through the method of the two port transmission/ reflection [18].

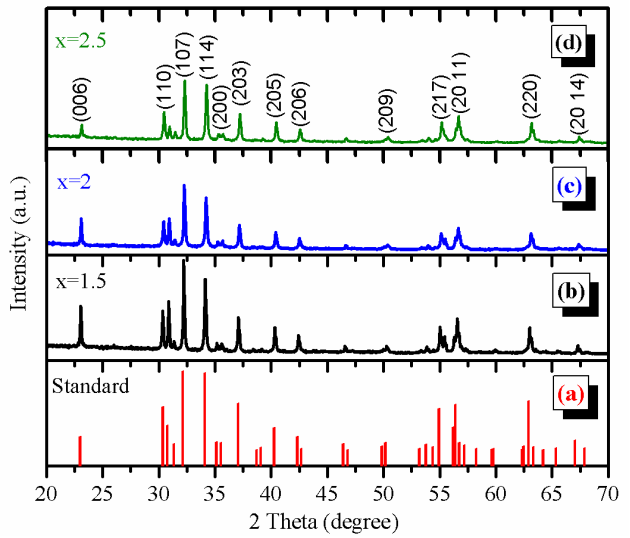

Fig. 1. X-ray diffraction patterns for M-type $BaFe_{12-x}(MnCo)_{0.5x}Ti_{0.5x}O_{19}$ (x=1.5, 2, 2.5) hexaferrite powders.

The relative complex permittivity and the relative complex permeability were calculated from S-parameters, according to ASTM D7449 standard. The reflection loss (RL) of a microwave absorbing layer with metal back is calculated based on the values of relative complex permeability and permittivity values in terms of frequency and thickness of layer by the following formulas [19]:

$$R.L. = -20log_{10}\left|\frac{Z_{in}-Z_0}{Z_{in}+Z_0}\right| \quad (1)$$

$$\frac{Z_{in}}{Z_0} = \sqrt{\frac{\mu_r}{\varepsilon_r}}tanh\left(j\frac{2\pi fd}{c}\sqrt{\mu_r\epsilon_r}\right) \quad (2)$$

where Z_{in} is the impedance of the composite, Z_0 is the intrinsic impedance of free space, d is the thickness of the absorber layer, c is the velocity of light in free space, f is the frequency of incident wave, μ_r is the relative permeability and ε_r is the relative permittivity of the composite layer [20].

3. Results and discussion

Fig. 1 shows the XRD pattern of the M-type $BaFe_{12-x}(MnCo)_{0.5x}Ti_{0.5x}O_{19}$ (x=1.5, 2, 2.5) hexaferrite samples. The pattern reveals that a single phase material was formed which indicated a high similarity to the standard XRD pattern of $BaFe_{12}O_{19}$ (JCPDS 007-0276) [21]. As can be seen, all compounds were of the single phase and there were almost no undesired phases in the patterns. So the ferrimagnetic phase were formed for all samples.

The morphologies and the particle size of samples were characterized by SEM. Some typical images are shown in Figure 2. The results showed that the distribution of particle size in various samples was wide and varied from about 100 nm to 1 μm. As shown in images, the particles highly tended to form aggregates. All of the compositions were sintered and crushed in a similar way, but obviously, average particle size decreases when the dopant content is increased. This may be explained on the basis that, with an increase in amount of dopants, more intermediate phase will be created and therefore, the formation of magnetoplumbite single phase will be complete at a higher temperature. It was concluded that porosity may be increased and crystallinity decreased in high level X. Hence, these porous powders are highly friable which facilitates easy grinding to obtain finer particles in high level substitution [22].

Fig. 3 shows the results of $BaFe_{12-x}(MnCo)_{0.5x}Ti_{0.5x}O_{19}$ (x=1.5, 2, 2.5) hexaferrites powders VSM measurements. The magnetic parameters are listed in Table 1. It can be clearly seen that the value of saturation magnetization was increased for x=2 and then decreased with increasing the amount of doping while the values of remanence and coercivity were continuously reduced by increasing the concentration of the dopants.

The magnetic properties of pure barium hexaferrite (BaM) have been variously reported because of the relationship with the method of synthesis, particle size, grain size, etc. Most of this research has recorded the value at around 72 emu/gr [5,6] at room temperature. It also has a high anisotropy constant, $K_1=3.3\times10^6$ erg/cm^3, which can give pure BaM a large crystalline anisotropy of 17 kOe (1352 kA/m) along the c-axis [5]. This uniaxial

character gives pure BaM a large theoretical maximum coercivity of 7.425 kOe (594 kA/m). A large number of works have been done to change the magnetic parameters of barium hexaferrite by substituting Fe^{3+} cations with other paramagnetic or diamagnetic cations [23]. A high value of H_c for undoped hexaferrite could be due to the strong uniaxial anisotropy along the c-axis of M-type hexaferrite. The reduction of coercivity for the doped hexaferrite could be because of the change in the easy axis of magnetization from the c-axis to the basal plane [24]. It is known that Fe^{3+} ions with up-spin are distributed on the 2a,12k and 2b sites, and ions with down-spin are located on the $4f_1$ and $4f_2$ sites [3]. It was found that the occupancy of the Mn-Co-Ti ions with down-spin on the $4f_1$ and $4f_2$ sites led to an increase in the net magnetization, and the occupancy of the *2a*, *12k* and *2b* sites gave rise to a decrease in the net magnetization. Therefore, increasing or decreasing saturation magnetization could be due to the different preference in site occupation of dopants by raising the amount of (x) when it substituted Fe^{+3} ions.

The reduction in the coercivity with increasing the amount of dopants(x) could be associated with the decrease in the anisotropy field as clearly shown in the following relation [7]. The measurement results are listed in Table 1.

$$H_c = C\,(H_a - N_d M_s) \qquad (3)$$

where C is a constant which depends on the nature and degree of the alignment of the magnetic particles, and N_d is the demagnetization factor, which depends on the shape of the particles.

It is worth noting that the slope of this reduction is not monotonic. It can be seen at x=2 that the slope of the H_c reduction is steeper than that at x=2.5. This observation may be because the replacement of iron ions at the $4f_1$ and $4f_2$ sites has a greater influence that at the12k site for magneto-crystalline anisotropy [9]. The order of anisotropy in barium ferrite for the Fe^{3+} occupied five-type holes should be $2b>4f_2>2b>4f_1>12k$ [25]. Therefore, the steep drop of H_c with lower substitution levels could be ascribed to the occupation of the $4f_2$ sites by Mn-Co-Ti dopants.

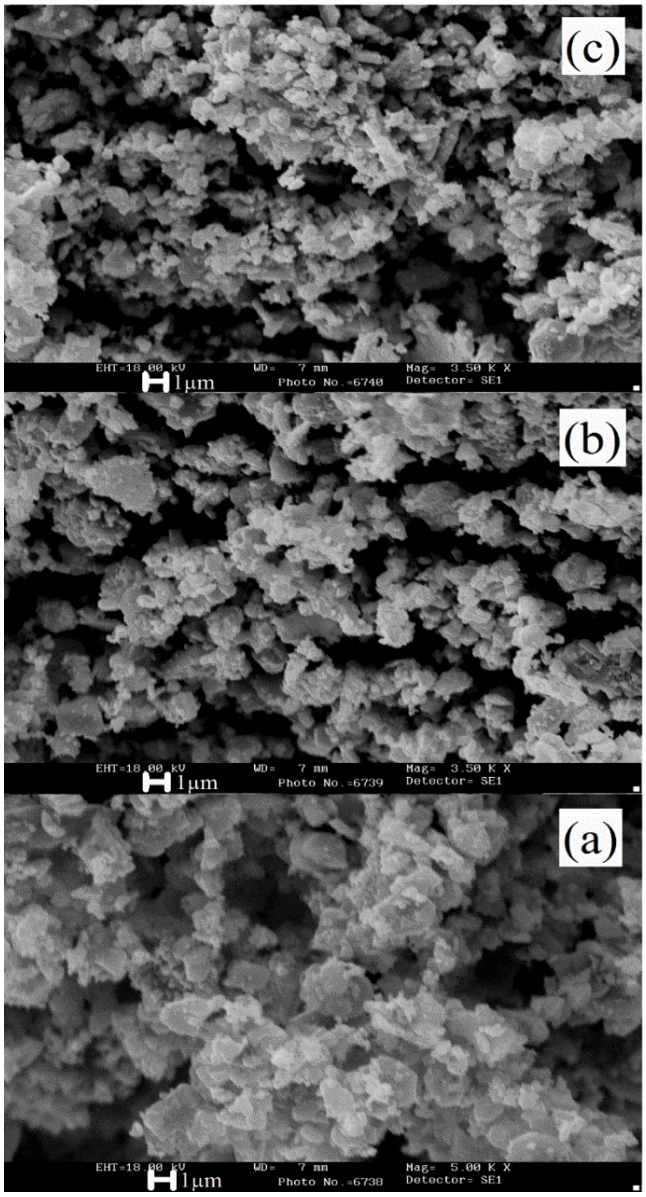

Fig 2. The SEM images of (a) x=1.5 (b) x=2 (c) x=2.5.

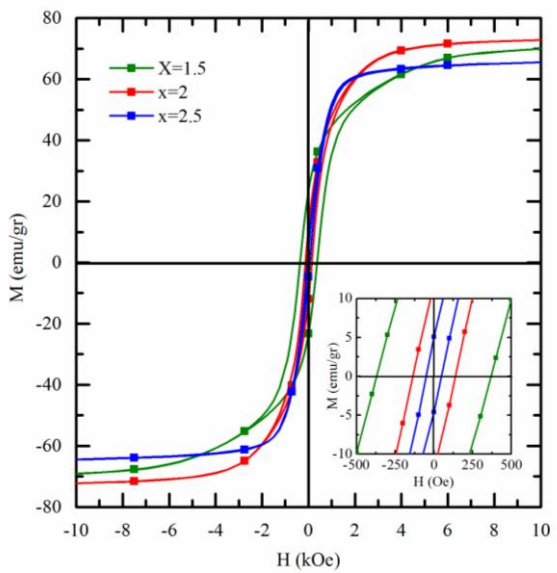

Fig. 3. M-H loops of $BaFe_{12-x}(MnCo)_{0.5x}Ti_{0.5x}O_{19}$ (x=1.5, 2, 2.5) hexaferrite powders at room temperature.

Table 1. Magnetic properties of $BaFe_{12-x}(MnCo)_{0.5x}Ti_{0.5x}O_{19}$ (x=1.5, 2, 2.5) hexaferrites powders at room temperature.

x	M_s (emu/gr)	M_r (emu/gr)	H_c (Oe)	FMR GHz	μ″(FMR)	-10 dB RL Bandwidth(GHz)		
						C-Band	X-Band	Ku-Band
1.5	70	24	370	18	0.37	--	--	0.85
2	73	12	137	11.4	0.37	--	1.3	3
2.5	66	7	49	5.6	0.45	2.3	1.4	--

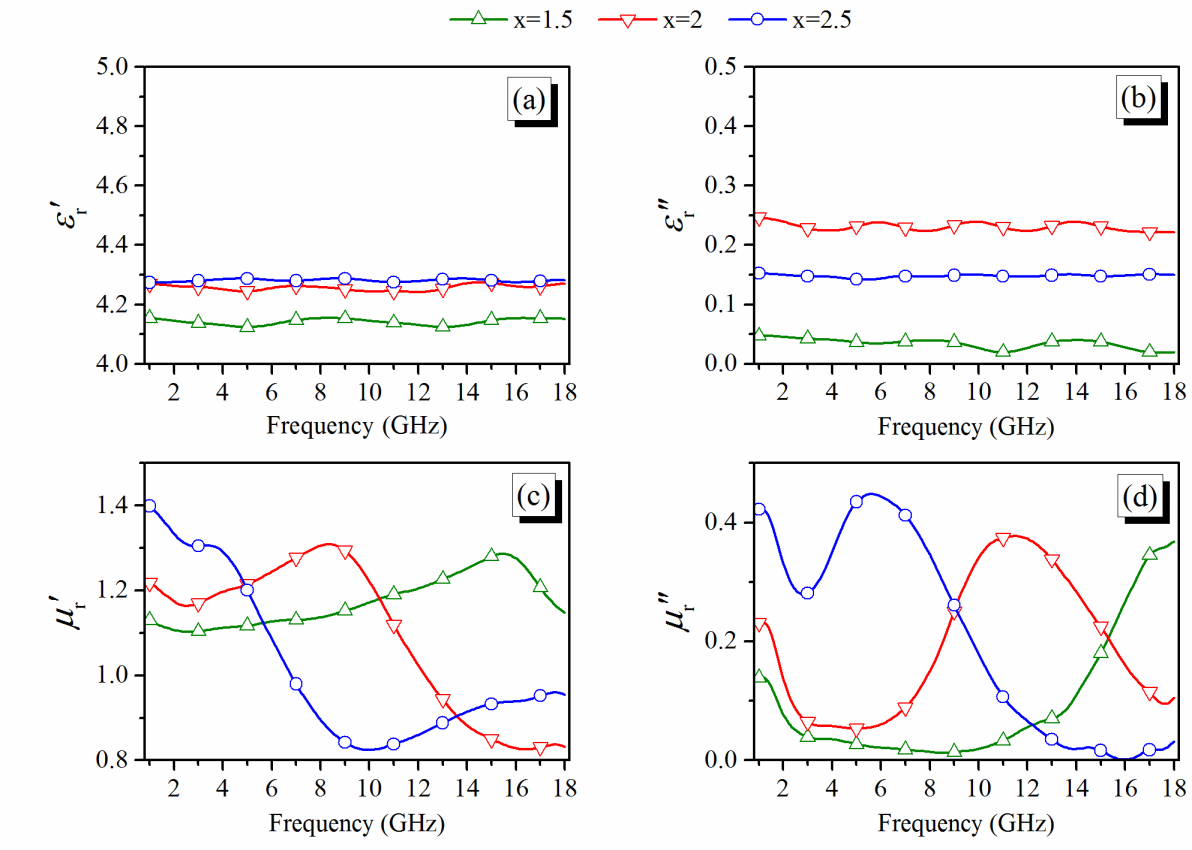

Fig. 4. Measured spectra of (a) the real part of relative permittivity, (b) the imaginary part of relative permittivity, (c) the real part of relative permeability and (d) the imaginary part of permeability for composite samples.

Fig. 4 shows complex relative permittivity and permeability spectra of the composite samples for different amounts of dopants. The ε_r'' values were increased by raising the amount of dopants while ε_r' demonstrated a slight change and weak frequency dependence within the frequency range. The conduction mechanism in ferrite could be attributed to the easy electron transfer between Fe^{2+} and Fe^{3+} as it had an effect on the permittivity. The permeability was related to the magnetic moments in material. This could be explained based on Gilbert-Wallace equation [26].

$$\mu_i = 1 + \frac{(4\pi M_S)^2}{(4\pi M_S)H_a - (f/2.8)^2 + j\alpha(4\pi M_S)(f/2.8)} \quad (4)$$

where μ_i is the intrinsic permeability, M_s is the saturation magnetization, H_a is the magnetocrystalline anisotropy, and f is the frequency. Based on the above relation, the decrease in anisotropy, besides the increase in M_s, plays a role in the increase in permeability. The ferromagnetic resonance (FMR) can be expressed by the following relation:

$$f_{FMR} = \left(\frac{\gamma}{2\pi}\right)^2 \left[(N_z - N_x)M_s + H_\theta^A\right]\left[(N_y - N_x)M_s + H_\varphi^A\right] \quad (5)$$

The external field is assumed to be the zero value. Also, N_x, N_y, and N_z are the demagnetization factors. M_s is the saturation magnetization. H_θ^A and H_φ^A are the out-of plane and in-plane anisotropy fields, respectively [27]. H_θ^A and H_φ^A are given by:

$$H_\theta^A = \frac{2K_\theta}{M_S} \quad (6)$$

and

$$H_\varphi^A = \frac{36K_\varphi}{M_S} \quad (7)$$

As noted before, the anisotropy filed is dramatically decreased by raising the amount of dopants. Consequently, H_θ^A and H_φ^A in equation (5) are decreased and then, the FMR might be reduced. This reduction in FMR can be clearly seen in Figure 4 (d). The relevant data for f_{FMR} and μ''_{FMR} are listed in Table 1. It is clearly seen that a peak for each composition at the beginning of the μ'' spectra can be attributed to magnetic domain wall resonance.

The optimal RL curves have been drawn for all three samples in Figure 5. These curves were calculated could find the optimal thickness for each material by receiving ε_r and μ_r complex coefficients in different frequency bands based on the maximum bandwidth and some RL intensity less than -10dB. Fig. 5 (a) shows that the sample with x=2.5 (4.5 mm thickness) presents efficient absorption with less than -10dB and 2.3 GHz bandwidth at C band frequency. As shown in Figure 5 (b), the samples with x=2 (3.2 mm thickness) and x=2.5 (4.1 mm thickness) represented the microwave absorption less than -10 dB and the bandwidth of 1.3 GHz and 1.4 GHz at X band frequency, respectively. Also, for sample with x=2 (2.6 mm thickness), the bandwidth of reflection loss with less than -10 dB was 3 GHz at Ku frequency. Therefore, the results demonstrated that $BaFe_{12-x}(MnCo)_{0.5x}Ti_{0.5x}O_{19}$ (x=1.5, 2, 2.5) composite materials could be applied as a microwave absorbing or shielding materials at different frequency bands.

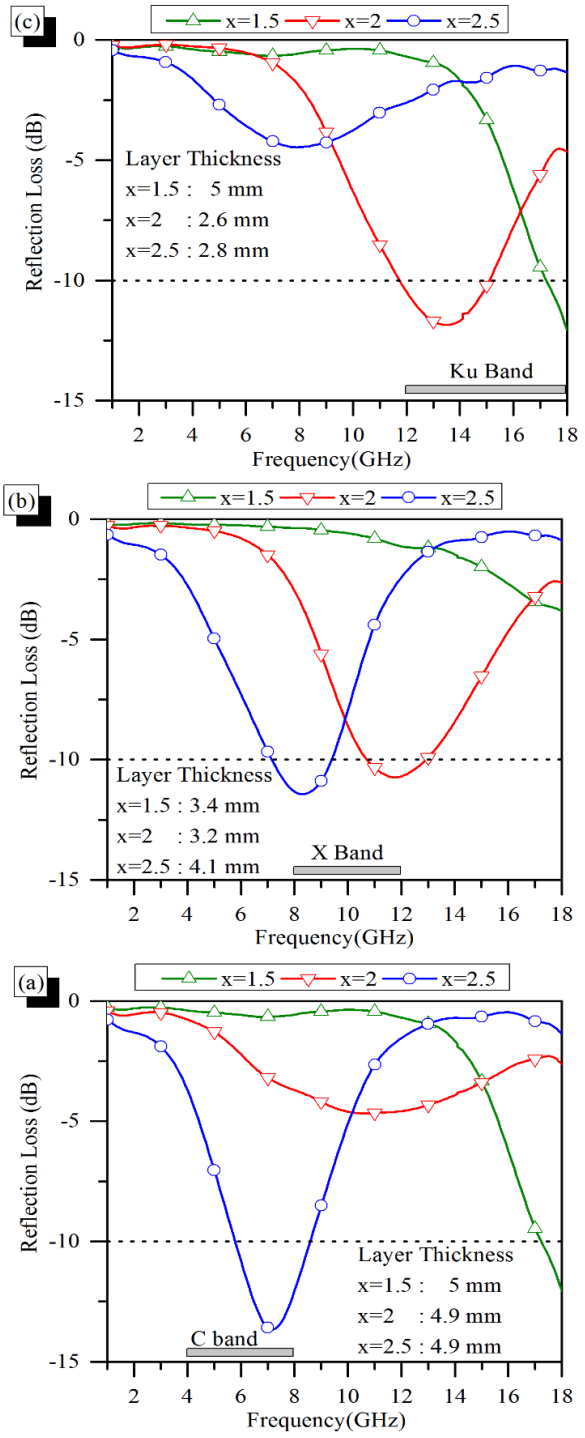

Fig. 5. Optimal RL plots of samples x=1.5, 2, and 2.5 in different frequency bands, (a) C band, (b) X band, and (e) Ku band

4. Conclusion

Single phase $BaFe_{12-x}(MnCo)_{0.5x}Ti_{0.5x}O_{19}$ (x=1.5, 2, 2.5) hexaferrites were prepared via the conventional ceramic method with the particle size of about 100 nm to 1 μm. The static magnetic characteristics of the substituted ferrites are presented. The saturation magnetization was increased for x=2 and then decreased with increasing the amount of doping while the values of remanence and coercivity were continuously reduced by increasing the concentration of the dopants. The complex permittivity and permeability were found to be controlled by tailoring the amount of the dopants. It can be therefore concluded that these compositions provide the microwave absorption in C, X and Ku-band frequencies. Reflection losses less than −10 dB were observed for all compositions in wideband frequency ranges.

Acknowledgements

The authors would like to thank the Office of Graduate Studies of the University of Isfahan for their support.

References

[1] Y. Guan, Y. Lin, L. Zou, Q. Miao, M. Zeng, Z. Liu, X. Gao,J. Liu, AIP Advances **3**, 2115 (2013).
[2] F. Qin,C. Brosseau, Journal of Applied Physics **111**, 061301 (2012).
[3] Ü. Özgür, Y. Alivov,H. Morkoç, Journal of Materials Science: Materials in Electronics **20**, 789 (2009).
[4] V. Šepelák, M. Myndyk, R. Witte, J. Röder, D. Menzel, R. Schuster, H. Hahn, P. Heitjans, K.-D. Becker, Faraday discussions **170**, 121 (2014).
[5] R. C. Pullar, Progress in Materials Science **57**, 1191 (2012).
[6] D. A. Vinnik, D. A. Zherebtsov, L. S. Mashkovtseva, S. Nemrava, A. S. Semisalova, D. M. Galimov, S. A. Gudkova, I. V. Chumanov, L. I. Isaenko, R. Niewa, Journal of Alloys and Compounds **628**, 480 (2015).
[7] A. Alsmadi, I. Bsoul, S. Mahmood, G. Alnawashi, K. Prokeš, K. Siemensmeyer, B. Klemke,H. Nakotte, Journal of Applied Physics **114**, 243910 (2013).
[8] E. Kiani, A. S. Rozatian,M. H. Yousefi, Journal of Magnetism and Magnetic Materials **361**, 25 (2014).
[9] M. Jazirehpour, M. Shams,O. Khani, Journal of Alloys and Compounds **545**, 32 (2012).
[10] S. Kanagesan, M. Hashim, S. Jesurani, T. Kalaivani, I. Ismail, Journal of Superconductivity and Novel Magnetism **27**, 811 (2014).
[11] I. Ali, M. Islam, M. Awan,M. Ahmad, Journal of Alloys and Compounds **547**, 118 (2013).
[12] S. Chawla, R. Mudsainiyan, S. Meena,S. Yusuf, Journal of Magnetism and Magnetic Materials **350**, 23 (2014).
[13] S. J. Harker, G. A. Stewart, W. D. Hutchison, A. Amiet,D. Tucker, Hyperfine Interact. **230**, 205 (2015).
[14] S. P. Gairola, V. Verma, A. Singh, L. P. Purohit, R. K. Kotnala, Solid State Communications **150**, 147 (2010).
[15] S. Choopani, N. Keyhan, A. Ghasemi, A. Sharbati, R. S. Alam, Materials Chemistry and Physics **113**, 717 (2009).
[16] S. Choopani, N. Keyhan, A. Ghasemi, A. Sharbathi, I. Maghsoudi,M. Eghbali, Journal of Magnetism and Magnetic Materials **321**, 1996 (2009).
[17] A. Ghasemi, A. Saatchi, M. Salehi, A. Hossienpour, A. Morisako,X. Liu, physica status solidi (a) **203**, 2513 (2006).
[18] J. Baker-Jarvis, E. J. Vanzura,W. A. Kissick, Microwave Theory and Techniques, IEEE Transactions on **38**, 1096 (1990).
[19] Z. Han, D. Li, M. Tong, X. Wei, R. Skomski, W. Liu, Z. Zhang,D. J. Sellmyer, Journal of Applied Physics **107**, 09A929 (2010).
[20] M. H. Shams, S. M. A. Salehi,A. Ghasemi, Materials Letters **62**, 1731 (2008).
[21] Joint Committee on Powder Diffraction, Standards (JCPDS) Powder Diffraction File (PDF), International Centre for Diffraction Data, Newtown Square, PA, (2004).
[22] Y.-P. Fu, K.-Y. Pan,C.-H. Lin, Materials Letters **57**, 291 (2002).
[23] P. Wartewig, M. Krause, P. Esquinazi, S. Rösler,R. Sonntag, Journal of magnetism and magnetic materials **192**, 83 (1999).
[24] S. Ruan, B. Xu, H. Suo, F. Wu, S. Xiang,M. Zhao, Journal of Magnetism and Magnetic Materials **212**, 175 (2000).
[25] Y. Liu, M. G. Drew,Y. Liu, Journal of Magnetism and Magnetic Materials **323**, 945 (2011).
[26] J. Jiang, L. Zhen, W. Shao,Z. Zhou, Journal of Applied Physics **112**, 053917 (2012).
[27] X. Li, R. Gong, Z. Feng, J. Yan, X. Shen,H. He, Journal of the American Ceramic Society **89**, 1450 (2006).

* Corresponding author: yousefimh40@gmail.com